

# Hadron collisions at ultrahigh energies: black disk or resonant disk modes?

V.V. Anisovich<sup>+</sup>, V.A. Nikonov<sup>+◇</sup> and J. Nyiri<sup>\*</sup>

May 6, 2019

<sup>+</sup>*National Research Centre "Kurchatov Institute", Petersburg Nuclear Physics Institute, Gatchina, 188300, Russia*

<sup>◇</sup> *Helmholtz-Institut für Strahlen- und Kernphysik, Universität Bonn, Germany*

<sup>\*</sup>*Institute for Particle and Nuclear Physics, Wigner RCP, Budapest 1121, Hungary*

## Abstract

The analysis of current ultrahigh energy data for hadronic total cross sections and diffractive scattering cross sections points to a steady growth of the optical density with energy for elastic scattering amplitudes in the impact parameter space,  $b$ . At LHC energy the profile function of the  $pp$ -scattering amplitude,  $T(b)$ , reaches the black disk limit at small  $b$ . Two scenarios are possible at larger energies,  $\sqrt{s} \gtrsim 100$  TeV. First, the profile function gets frozen in the black disk limit,  $T(b) \simeq 1$  while the radius of the black disk  $R_{black\ disk}$  is increasing with  $\sqrt{s}$ , providing  $\sigma_{tot} \sim \ln^2 s$ ,  $\sigma_{el} \sim \ln^2 s$ ,  $\sigma_{inel} \sim \ln^2 s$ . In another scenario the profile function continues to grow at  $\sqrt{s} \gtrsim 100$  TeV approaching the maximal value,  $T(b) \simeq 2$ , that means the resonant disk mode. We discuss features of the resonant disk mode when the disk radius,  $R_{resonant\ disk}$ , increases providing the growth of the total and elastic cross sections  $\sigma_{tot} \sim \ln^2 s$ ,  $\sigma_{el} \sim \ln^2 s$ , but a more slow increase of inelastic cross section,  $\sigma_{inel} \sim \ln s$ .

PACS: 13.85.Lg 13.75.Cs 14.20.Dh

## 1 Introduction

The data [1, 2] definitely confirm the previous observations [3], namely, that the total cross sections increase steadily with energy ( $\sigma_{tot} \sim \ln^n s$  as  $1 \lesssim n \lesssim 2$ ); the steady growth is observed for  $\sigma_{el}$  and  $\sigma_{inel}$ , while the ratio  $ReA_{el}/ImA_{el}$  is small and probably decreases slowly.

Already the first indications of the cross sections growth [4] gave start to corresponding models with the supercritical pomeron [5, 6]. The concept of the power growth of cross sections ( $\sigma_{tot} \sim s^\Delta$  with  $\Delta \simeq 0.08$ ) became widely accepted in the 1980s [7, 8] and is discussed till now [9] (let us note that exceeding of the Froissart bound [10] does not violate necessarily the general constraints [11]).

It was shown in [12, 13, 14] that the power-type growth of scattering amplitudes is dumped to  $\ln^2 s$ -type within the  $s$ -channel unitarization. The black disk picture with the  $\ln^2 s$ -growth of the  $\sigma_{tot}$  and  $\sigma_{el}$  at ultrahigh energies was suggested in the Dakhno-Nikonov model [15]. The model can be considered as a realization of the Good-Walker eikonal approach [16] for a continuous set of channels. Presently, the black disk mode for hadron collisions at ultrahigh energies is discussed extensively, see, for example, [17, 18, 19, 20, 21, 22, 23, 24, 25].

The black disk mode is usually discussed in terms of the optical density for elastic scattering amplitude. For the asymptotic regime such a presentation was carried out in [26, 27]: the cross sections  $\sigma_{tot}(pp)$ ,  $\sigma_{el}(pp)$ ,  $\sigma_{inel}(pp)$  demonstrate a maximal growth,  $\sim \ln^2 s$ , while diffractive dissociation cross sections  $\sigma_D(pp)$ ,  $\sigma_{DD}(pp)$  give a slower growth,  $\sim \ln s$ .

For the calculation of screening corrections in inelastic diffractive processes at ultrahigh energies [28] the  $K$ -matrix technique is more preferable. The  $K$ -matrix function  $-iK(b)$  in the preLHC region increases with energy being mainly concentrated at  $b < 1$  fm. The black disk regime for the  $K$ -matrix function means its "freezing",  $-iK(b) \rightarrow 1$ , in the disk area. If the growth of the  $-iK(b)$  continues with increasing energy, the interaction area turns into a resonant disk. In this case asymptotically  $\sigma_{tot}(pp) \sim \ln^2 s$ ,  $\sigma_{el}(pp) \sim \ln^2 s$  with  $[\sigma_{el}(pp)/\sigma_{tot}(pp)]_{s \rightarrow \infty} \rightarrow 1$ ; the resonant disk area is surrounded by a black border band that provides  $\sigma_{inel}(pp) \sim \ln s$ ,  $\sigma_D(pp) \sim \ln s$ ,  $\sigma_{DD}(pp) \sim \ln s$ .

In the present paper we perform a comparative analysis of predictions for ultrahigh energy diffractive processes in the framework of these two scenarios. It is definitely seen that the data at  $\sqrt{s} \sim 10$  TeV are not sensitive to the versions of the disk: the initial stages are similar in both modes. Distinctions are seen at  $\sqrt{s} \sim 10^3 - 10^4$  TeV. Apparently, the study and interpretation of the cosmic ray data at such energies are the problems on the agenda.

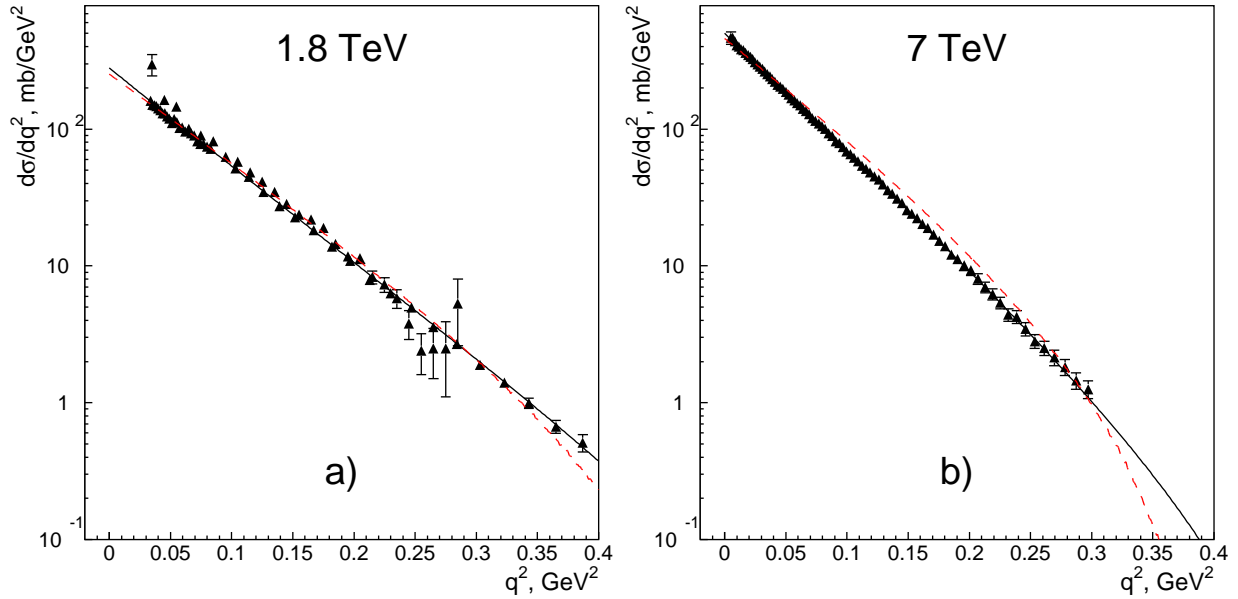


Figure 1: a,b) Differential cross sections  $d\sigma_{el}/dq^2$  at  $\sqrt{s} = 1.8, 7.0$  TeV and their description within the black disk mode (red dashed lines) and the resonant disk mode (solid lines).

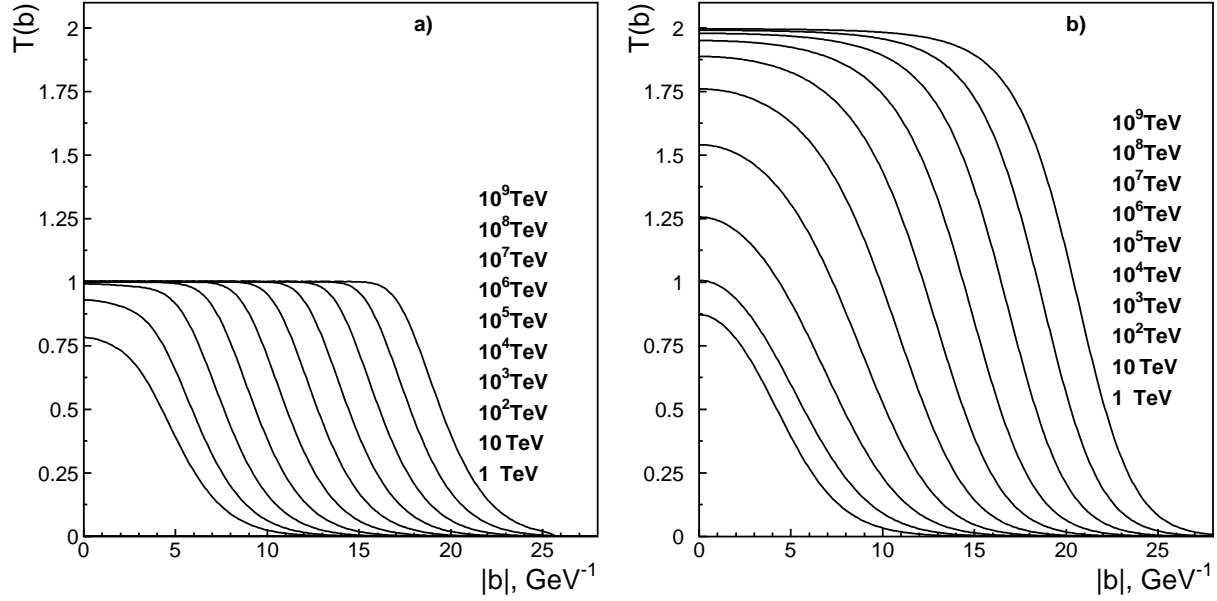


Figure 2: a) Profile functions,  $T(b)$ , at  $\sqrt{s} = 1, 10, 10^2, \dots, 10^9$  TeV for the black disk regime ( $T(b) \rightarrow 1$ ) and b) resonant disk regime ( $T(b) \rightarrow 2$ ). At  $\sqrt{s} = 1 - 10$  TeV the profile functions in both modes are nearly the same.

## 2 Scattering amplitude in the impact parameter space and the K-matrix representation for ultrahigh energy

In the impact parameter space the profile function  $T(b)$  is determined at high energies as:

$$\begin{aligned} \sigma_{tot} &= 2 \int d^2b T(b), \\ 4\pi \frac{d\sigma_{el}}{d\mathbf{q}_\perp^2} &= |A_{el}(\mathbf{q}_\perp^2)|^2, \quad A_{el}(\mathbf{q}_\perp^2) = i \int d^2b e^{i\mathbf{b}\mathbf{q}_\perp} T(b), \\ T(b) &= 1 - \eta(b) e^{2i\delta(b)} = 1 - e^{-\frac{1}{2}\chi(b)} = \frac{-2iK(b)}{1 - iK(b)}, \end{aligned} \tag{1}$$

here  $A_{el}(\mathbf{q}_\perp^2)$  is the elastic scattering amplitude. The profile function can be presented either in the standard form using the inelasticity parameter  $\eta(b)$  and the phase shift  $\delta(b)$  or in terms of the optical density  $\chi(b)$  and the K-matrix function  $K(b)$ . The K-matrix approach is based on the separation of the elastic rescatterings in the intermediate states: the function  $K(b)$  includes only the multiparticle states thus being complex valued. The small value of the  $ReA_{el}/ImA_{el}$  tells that  $K(b)$  is dominantly imaginary.

### 2.0.1 Black disk limit in terms of the Dakhno-Nikonov model

The Dakhno-Nikonov model [15] demonstrates us a representative example of application of the optical density technique for the consideration of  $pp^\pm$  collisions at ultrahigh energies when  $\ln s \gg 1$ . In the model the black disk is formed by the low density pomeron cloud and rescatterings are described within the eikonal approach. The scattering amplitude  $AB \rightarrow AB$

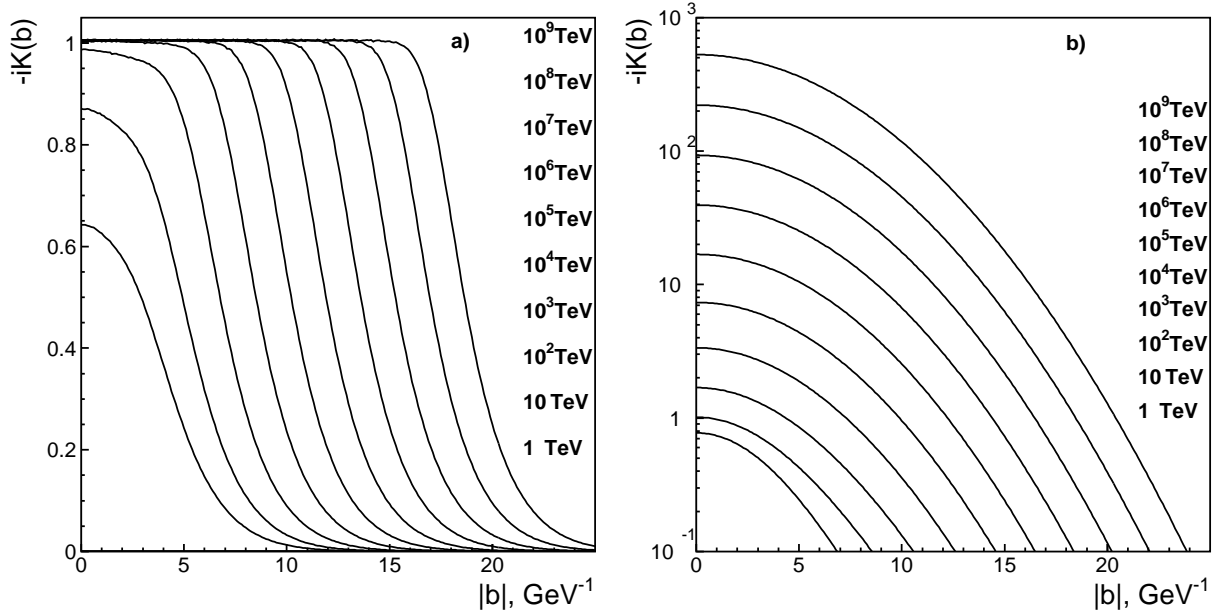


Figure 3: The K-matrix functions,  $-iK(b)$ , for a) the black disk mode ( $[-iK(b)]_{\xi \rightarrow \infty} \rightarrow 1$  at  $b < R_0 \xi$ ) and b) the resonant disk mode ( $[-iK(b)]_{\xi \rightarrow \infty} \rightarrow \infty$  at  $b < R_0 \xi$ ).

reads:

$$A_{AB \rightarrow AB}(\mathbf{q}^2) = i \int d^2 b e^{i\mathbf{q}\mathbf{b}} \int dr' \varphi_A^2(r') dr'' \varphi_B^2(r'') \left[ 1 - \exp \left( -\frac{1}{2} \chi_{AB}(r', r'', \mathbf{b}) \right) \right], \quad (2)$$

where  $dr \varphi_A^2(r)$ ,  $dr \varphi_B^2(r)$  are the quark densities of the colliding hadrons in the impact parameter space. Proton and pion quark densities can be determined using the corresponding form factors. The optical density  $\chi_{AB}(r', r'', \mathbf{b})$  depends on parameters of the  $t$ -channel interaction.

The behavior of amplitudes at ultrahigh energies is determined by leading complex- $j$  singularities, in the Dakhno-Nikonov model that are leading and next-to-leading pomerons with trajectories  $\alpha(\mathbf{q}^2) \simeq 1 + \Delta - \alpha' \mathbf{q}^2$ . The fit of refs. [22, 26] gives:

parameters	leading pole	next-to-leading
$\Delta$	0.27	0
$\alpha'_P [(\text{GeV})^{-2}]$	0.13	0.25

(3)

In terms of the K-matrix approach the black disk mode means the assumed freezing of the  $-iK(b)$  in the interaction area:

$$\begin{aligned} \left[ -iK(b) \right]_{\xi \rightarrow \infty} &\rightarrow 1 && \text{at } b < R_0 \xi, \\ \left[ -iK(b) \right]_{\xi \rightarrow \infty} &\rightarrow 0 && \text{at } b > R_0 \xi, \end{aligned} \quad (4)$$

$$\xi = \ln \frac{s}{s_R}, \quad s_R \simeq 6.4 \cdot 10^3 \text{ GeV}^2, \text{ with } R_0 \simeq 2\sqrt{\alpha' \Delta} \simeq 0.08 \text{ fm}.$$

The growth of the radius of the black disk is slow: the small value of  $R_0$  is caused by the large mass of glueballs [29, 30] and the effective mass of gluons [31, 32].

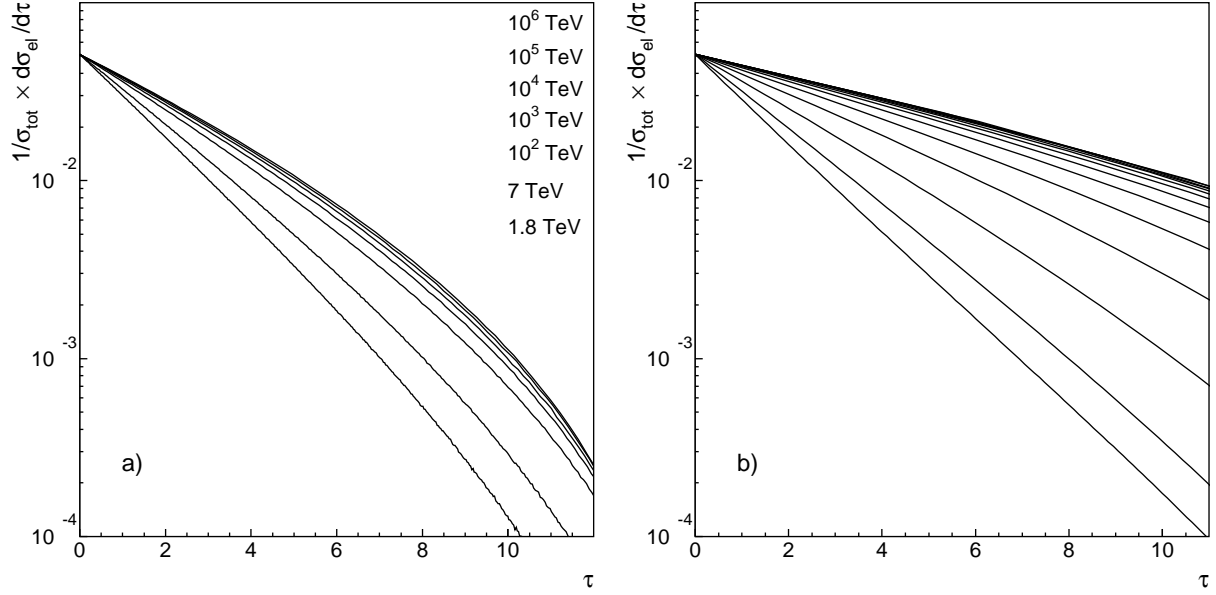


Figure 4: The black disk (a) and resonant disk (b) modes: the  $\tau$ -representation ( $\tau = \sigma_{tot} \mathbf{q}^2$ ) for differential cross section,  $\frac{1}{\sigma_{tot}} \frac{d\sigma_{el}}{d\tau}$ . The differential cross sections are similar at  $\sqrt{s} = 1.8, 7$  TeV; distinctions are seen at  $\sqrt{s} \geq 10^3$  TeV.

The black disk mode results in

$$\begin{aligned} \sigma_{tot} &\simeq 2\pi(R_0\xi)^2, \\ \sigma_{el} &\simeq \pi(R_0\xi)^2, \quad \sigma_{inel} \simeq \pi(R_0\xi)^2. \end{aligned} \quad (5)$$

For the black disk radius the corrections of the order of  $\ln \xi$  exist  $R_{black\ disk} \simeq R_0\xi + \varrho \ln \xi$  but they become apparent in the Dakhno-Nikonov model at energies of the order of the Plank mass,  $\sqrt{s} \sim 10^{17}$  TeV.

### 2.0.2 Resonant disk and K-matrix function

From the data it follows that both  $T(b)$  and  $-iK(b)$  are increasing with energy, being less than unity. If the eikonal mechanism does not quench the growth, both characteristics cross the black disk limit getting  $T(b) > 1$ ,  $-iK(b) > 1$ . If  $-iK(b) \rightarrow \infty$  at  $\ln s \rightarrow \infty$ , which corresponds to a growth caused by the supercritical pomeron ( $\Delta > 0$ ), the diffractive scattering process gets to the resonant disk mode.

For following the resonant disk switch-on we use the two-pomeron model with parameters providing the description of data at 1.8 TeV and 7 TeV, namely:

$$\begin{aligned} -iK(b) &= \int \frac{d^2q}{(2\pi)^2} \exp(-i\mathbf{qb}) \sum g^2 s^\Delta e^{-(a+\alpha\xi)\mathbf{q}^2} \\ &= \sum \frac{g^2}{4\pi(a+\alpha'\xi)} \exp\left[\Delta\xi - \frac{\mathbf{b}^2}{4(a+\alpha'\xi)}\right], \quad \xi = \ln \frac{s}{s_0}. \end{aligned} \quad (6)$$

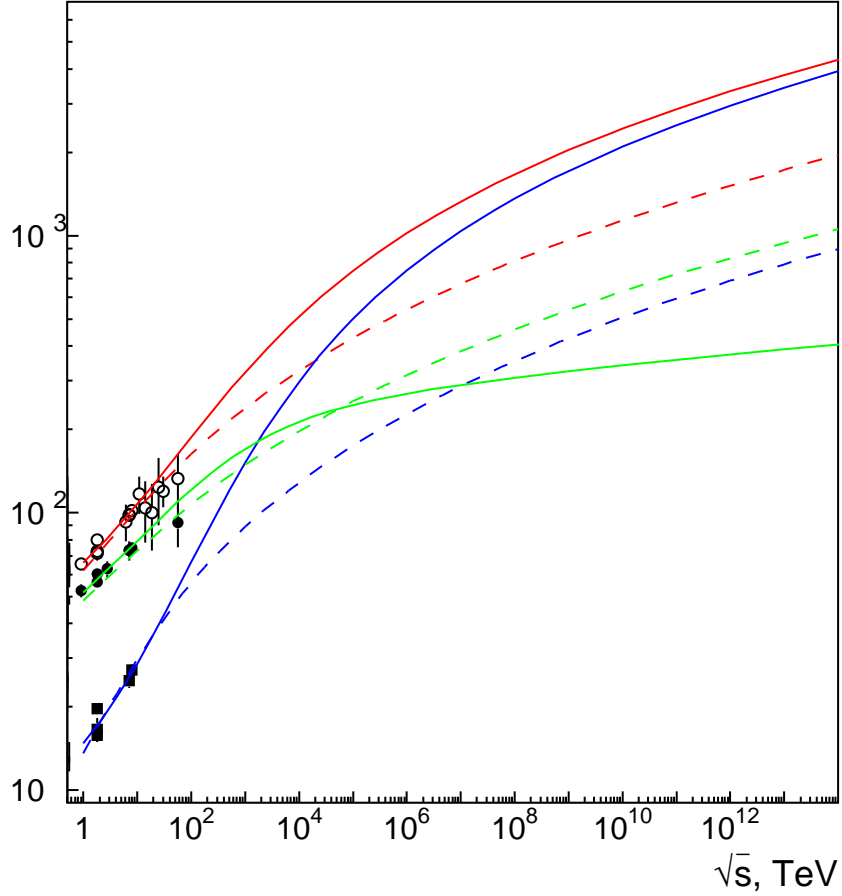


Figure 5: Total, elastic and inelastic cross sections for resonant disk (solid lines) and black disk (dashed lines) modes: red  $\sigma_{tot}$ , blue  $\sigma_{el}$ , green  $\sigma_{inel}$ .

The following parameters are found for the leading and the next-to-leading pomerons:

parameters	leading pole	next-to-leading
$\Delta$	0.20	0
$\alpha'_P$ [GeV <sup>-2</sup> ]	0.18	0.14
$a$ [GeV <sup>-2</sup> ]	6.67	2.22
$g^2$ [mb]	1.74	28.6
$s_0$ [GeV <sup>2</sup> ]	1	1

(7)

The description of the differential cross sections  $d\sigma_{el}/d\mathbf{q}_\perp^2$  at  $\sqrt{s} = 1.8, 7.0$  TeV in resonant disk mode is demonstrated in Fig. 1. The resonant interaction regime occurs at  $b < 2\sqrt{\alpha'\Delta}\xi = R_0\xi$ , in this region  $T(b) \rightarrow 2$ . In terms of the inelasticity parameter and the phase shift it corresponds to  $\eta \rightarrow 1$  and  $\delta \rightarrow \pi/2$ . Cross sections at  $\xi \rightarrow \infty$  obey  $\sigma_{tot} \simeq 4\pi R_0^2\xi^2$ ,  $\sigma_{el}/\sigma_{tot} \rightarrow 1$  and  $\sigma_{inel} \simeq 2\pi R_0\xi$ .

### 2.0.3 Comparative survey of the resonant disk and black disk modes

At the energy  $\sqrt{s} \sim 10$  TeV the black cloud fills out the proper hadron domain, the region  $\leq 1$  fm, and that happens in both modes. It is demonstrated in Figs. 2,3: the profile functions

$T(b)$  coincide practically in both modes as well as the K-functions  $-iK(b)$ . Correspondingly, the differential cross sections in  $\tau$ -representation differ a little, mainly at  $\tau \sim 10$ , Fig. 4. The energy behavior of  $\sigma_{tot}$ ,  $\sigma_{el}$  and  $\sigma_{inel}$  coincide also at  $\sqrt{s} \sim 1 - 100$  TeV in both modes, Fig. 5.

Differences appear at  $\sqrt{s} \sim 1000$  TeV:  $T(b) \simeq 1.5$  at  $b \lesssim 0.5$  fm and the black zone has shifted to  $b \simeq 1.0 - 1.5$  fm, Fig. 3b. With further energy increase the radius of the black band increases as  $2\sqrt{\Delta\alpha'\xi} \equiv R_{rd}\xi$ . The rate of growth in both modes is determined by the leading singularity and the fit of the data in the region  $\sqrt{s} \sim 1 - 10$  TeV gives approximately the same values of  $\Delta$  and  $\alpha'$  for both cases thus providing  $R_0 \simeq R_{rd}$ .

### 3 Conclusion

The interaction of soft gluons determines the physics of hadrons. The effective gluons are massive and their mass is of the order of 1 GeV that is seen directly in radiative decays of heavy quarkonia [31, 32],  $\psi \rightarrow \gamma + \text{hadrons}$  and  $\Upsilon \rightarrow \gamma + \text{hadrons}$ . The effective gluon mass is determinative both for low energy physics, making possible to introduce the notion of the constituent quark, and for high energy physics, dictating the rate of the growth of the interaction radius. High energy physics is the physics of large logarithms,  $\ln s/s_0 \gg 1$ , and the value  $\sqrt{s_0} \sim m_{\text{effective gluon}}$  corresponds to a start of the asymptotic regime at  $\sqrt{s} \sim 1$  TeV. However, the initial increments of the measured characteristics such as  $\sigma_{tot}$ ,  $\sigma_{el}$  and  $\sigma_{inel}$  are visually similar, and therefore their behavior in this region does not distinguish between different versions. A real discrimination of modes can appear when cross section data are discussed at much larger energies,  $\sqrt{s} \sim 10^3 - 10^4$  TeV.

Cosmic ray data probably can provide information to fix asymptotic mode. Another way is to study the diffractive inelastic processes which differ strongly for different modes [28].

### Acknowledgment

We thank M.G. Ryskin and A.V. Sarantsev for useful discussions and comments. The work was supported by grants RFBR-13-02-00425 and RSGSS-4801.2012.2.

### References

- [1] G. Latino [on behalf of TOTEM Collaboration], EPJ Web Conf. **49**, 02005 (2013) [arXiv:1302.2098 [hep-ex]].
- [2] Pierre Auger Collaboration (P. Abreu *et al.*), Phys. Rev. Lett. **109**, 062002 (2012).
- [3] UA4 Collaboration, Phys. Lett. **B147**, 385 (1984);  
 UA4/2 Collaboration, Phys. Lett. **B316**, 448 (1993);  
 UA1 Collaboration, Phys. Lett. **B128**, 336 (1982);  
 E710 Collaboration, Phys. Lett. **B247**, 127 (1990);  
 CDF Collaboration, Phys. Rev. **D50**, 5518 (1994).
- [4] Y.P. Gorin *et al.* Yad. Phys. **14**, 998 (1971).

- [5] A. Capella and J. Kaplan, Phys. Lett. **B52**, 448 (1974).
- [6] P.E. Volkovitsky, M.A. Lapidus, V.I. Lisin, K.A. Ter-Martirosyan, Yad. Phys. **24**, 1237 (1976).
- [7] A. Donnachie and P.V. Landshoff, Nucl. Phys. **B231**, 189 (1984).
- [8] A.B. Kaidalov and K.A. Ter-Martirosyan, Sov. J. Nucl. Phys. **39**, 979 (1984).
- [9] A. Donnachie and P.V. Landshoff, arXiv:11122485, (2011) [hep-ph].
- [10] M. Froissart, Phys. Rev. **123**, 1053 (1961).
- [11] Y.I. Azimov, Phys. Rev. **D84**, 056012 (2011); arXiv:1208.4304(2012) [hep-ph].
- [12] T.K. Gaisser and T. Stanev, Phys. Lett., **B219**, 375, 1989.
- [13] M. Block, F. Halzen and B. Margolis, Phys. Lett., **B252**, 481, 1990.
- [14] R.S. Fletcher, Phys. Rev. **D46**, 187, 1992.
- [15] L.G. Dakhno and V.A. Nikonov, Eur. Phys. J. **A8**, 209 (1999).
- [16] M.L. Good, W.D. Walker, Phys. Rev. **120**, 1857 (1960).
- [17] F. Halzen, K. Igi, M. Ishida and C.S. Kim, Phys. Rev. **D85**, 074020 (2012); arXiv:1110.1479V2(2012) [hep-ph].
- [18] V. Uzhinsky and A. Galoyan, arXiv:1111.4984v5(2012) [hep-ph].
- [19] M.G. Ryskin, A.D. Martin and V.A. Khoze, Eur. Phys. J. **C72**, 1937(2012); arXiv:1201.6298v2(2012) [hep-ph].
- [20] I.M. Dremin, V.A. Nechitailo, Phys. Rev. **D85**, 074009 (2012); arXiv:1202.2016 (2012) [hep-ph].
- [21] M.M. Block and F. Halzen, Phys. Rev. **D86**, 0501504 (2013); arXiv:1208.4086v1 (2012) [hep-ph].
- [22] V.V. Anisovich, K.V. Nikonov, and V.A. Nikonov, Phys. Rev. **D88**, 014039 (2013); [arXiv:1306.1735 [hep-ph]].
- [23] A. Alkin, E. Martynov, O. Kovalenko and S. M. Troshin, Phys. Rev. **D89**, 091501 (2014) [arXiv:1403.8036 [hep-ph]].
- [24] S. M. Troshin and N. E. Tyurin, Int. J. Mod. Phys. **A22**, 4437 (2007) [hep-ph/0701241].
- [25] M. Giordano and E. Meggiolaro, JHEP **1403**, 002 (2014) [arXiv:1311.3133 [hep-ph]].
- [26] V.V. Anisovich, V.A. Nikonov, and J. Nyiri, Phys. Rev. **D88**, 014039 (2013); [arXiv:1310.2839 (hep-ph)].
- [27] V.V. Anisovich, K.V. Nikonov, V.A. Nikonov and J. Nyiri, Int. J. Mod. Phys. **A29**, 1450096 (2014); arXiv:1404.1904 (hep-ph).



- [28] V.V. Anisovich, M.A. Matveev, and V.A. Nikonov, *Hadron diffractive production at ultra-high energies*, arXiv:1407.4588 (hep-ph).
- [29] V.V. Anisovich, AIP Conf. Proc. **619**, 197 (2002), **717**, 441 (2004); Phys.Usp. **47**, 45 (2004), [UFN **47**, 49 (2004)].
- [30] V.V. Anisovich, M.A. Matveev, J. Nyiri, A.V. Sarantsev, Int. J. Mod. Phys. **A20**, 6327 (2005).
- [31] G. Parisi and R. Petronzio, Phys. Lett. **94**, 51 (1980).
- [32] M. Consoli and J.H. Field, Phys. Rev. **D49**, 1293 (1994).